British Journal of Hospital Medicine

Br. J. Hosp. Med. (Lond) **2026**; 87(8): 49951
https://doi.org/10.31083/BJHM49951

Article

Predicting Coronary Artery Stenosis Severity in Coronary Heart Disease: A Combined Model of Triglyceride-Glucose Index and Carotid Ultrasound Radiomics

Haotian Hu[1], Runyu Zhu[1], Dian Shen[1], Aoyi Zhang[1], Wenshu Hu[1], Xinyi Li[1], Chang Zhou[1,*]

[1]Department of Ultrasound, The First College of Clinical Medical Science, China Three Gorges University and Yichang Central People's Hospital, 443000 Yichang, Hubei, China

*Correspondence: zhouchang1243@163.com (Chang Zhou)

Academic Editor: Sudarshan Ramachandran

Submitted: 12 January 2026 Revised: 4 April 2026 Accepted: 6 May 2026 Published: 21 August 2026

Abstract

Aims/Background: Precise evaluation of coronary lesion severity is pivotal for the clinical management of coronary heart disease (CHD). However, because the invasive coronary angiography (ICA) method, which is considered the gold standard for diagnosis, is relatively invasive, it is not widely used in early risk stratification. This study evaluated the performance of a predictive model based on a combined triglyceride-glucose (TyG) index and ultrasound radiomics characteristics of carotid plaques for evaluating coronary artery lesion severity in patients with CHD. **Methods:** From January 2020 to October 2024, 381 CHD patients were diagnosed by ICA at Yichang Central People's Hospital. Radiomics features were extracted from manually divided regions of interest (ROIs) in carotid plaque ultrasound images. A two-stage feature selection was carried out to identify the essential features, and then logistic regression was employed to construct a radiomics score (Rad score). Clinical data, such as the TyG index, were also included in the construction of the combined prediction model, and the predictive performance of this model was evaluated on both the training and test sets. **Results:** Multivariate logistic regression shows that the TyG index (odds ratio [OR] = 3.82, 95% confidence interval [CI]: 2.13–6.84), sex (OR = 1.80, 95% CI: 1.08–3.00), and hypertension status (OR = 1.81, 95% CI: 1.14–2.87) are all independent predictors of coronary lesion severity. Based on 17 essential radiomics features, the Rad score model reached an area under the curve (AUC) of 0.673 (95% CI: 0.613–0.734) for the training set and an AUC of 0.686 (95% CI: 0.567–0.806) for the test set. The combined model including sex, TyG index, hypertension status, and Rad score performed better, with AUC values of 0.823 (95% CI: 0.777–0.870) for the training set and 0.730 (95% CI: 0.616–0.844) for the test set. **Conclusion:** The combined model of the TyG index and ultrasound radiomics features for carotid plaques can be used to predict the severity of coronary artery lesions in patients with CHD. Non-invasively, it can be used to assess the risk of coronary artery disease and tailor a plan for other treatment options.

Keywords: radiomics; carotid ultrasound; coronary heart disease; carotid plaque; triglyceride-glucose index

1. Introduction

Coronary artery disease (CAD) is a long-term heart disease that occurs when there is narrowing in the coronary arteries, and it is generally caused by coronary heart disease (CHD). In recent years, due to changes in lifestyle and environment, more and more young people have been suffering from CHD [1,2]. Therefore, a new problem of public health has arisen. From 2010 to 2020, based on the above data, the annual increase in deaths from CHD in people aged 25–49 was 0.6%. The increase was relatively larger in poor countries and reached 1.2% [3]. As one of the world's serious health problems, CHD treatment relies on knowing how serious a person's heart disease is [4]. Invasive coronary angiography (ICA) is now a first-line diagnostic test for CHD. It can precisely locate atherosclerotic plaques and study the blood flow conditions at these sites [5]. However, ICA has several deficiencies and cannot be used widely. They are invasive, exposed to radiation, high in cost, and carry other procedural risks. As a result, there is a strong and urgent need in the clinic for such non-invasive, high-efficacy tools. ICA are used to observe how far the coronary arteries have been damaged and assess a person's risk. The problems of ICA are not the only reasons for this lack, and so are the realities of current clinical work.

Triglyceride-glucose (TyG) index is a new metabolic index. It is equal to the natural logarithm of the product of fasting triglycerides (TG, mg/dL) and fasting blood glucose (FBG, mg/dL) divided by two [ln(TG×FBG/2)]. A suitable index for insulin resistance and other metabolic diseases has been selected. A study has shown that, compared with the older method of diagnosis for insulin resistance (IR), the TyG index is comparatively simple and low in cost. Therefore, it can be used to classify metabolic risk [6]. As evidence, it has been shown that a high TyG level is strongly correlated with the onset of cardiovascular

disease [7,8]. The TyG index is now used to measure how poorly controlled the disease of atherosclerosis is in clinical practice. It relates to the extent of the disease and prolonged survival. Higher TyG indices in individuals are associated with an increased risk of CAD. They are also more likely to have severe coronary artery disease and poorer clinical outcomes compared with those with lower TyG values [9]. Based on the above results, the TyG index can be used to determine the extent of coronary artery disease in people with coronary heart disease. Thus, it is an index of non-invasive risk assessment. Therefore, in time, some high-risk patients may be identified early on for personalised treatments and better results.

Heart disease and other diseases of the blood vessels are caused by atherosclerosis. It is a general state of many blood vessels in the body. Carotid and coronary atherosclerosis are two types of the spread of this disease. They have a close relationship in epidemiology, the underlying pathological mechanisms, and clinical outcomes [10]. Notably, an increase in carotid intima-media thickness (CIMT) or the appearance of carotid plaques is closely linked to more serious coronary artery disease [11]. Fuster V et al. [12] have shown in their research that, as shown by carotid ultrasound noninvasively, the amount of carotid plaque is positively associated with the development and severity of coronary atherosclerosis over time, as well as other adverse health outcomes. Thus, the carotid artery may serve as a practical "window" to assess the risk of coronary atherosclerosis in a person. It is convenient for clinical applications, and therefore can provide data to help regulate all-around cardiovascular risk control.

Radiomics is a new field of artificial intelligence (AI) and medicine that extracts rich features from medical images. To uncover the underlying disease in the tissues that are not visible to the naked eye. We have built a model in this paper for predicting the degree of coronary artery stenosis. We combined the TyG index and radiomics features from carotid ultrasound. The study combines metabolic data and imaging data to explore the relationship between them in the disease of atherosclerosis and assesses the clinical effectiveness of the model. We will also explore some non-invasive applications of this study. The above tool can help to develop a rehabilitation plan for coronary heart disease. The combined model of operation is expected to be more all-encompassing in assessing the risks of both types of data.

2. Methods

2.1 Study Population

A retrospective study was conducted on consecutive patients with CHD who underwent ICA at Yichang Central People's Hospital from January 2020 to October 2024. The inclusion criteria were as follows: (1) Clinically diagnosed with CHD based on ICA results; (2) Underwent carotid artery ultrasound examination showing carotid plaque within 24 hours of ICA. The reasons for exclusion were: (1) Patients who had a history of percutaneous coronary intervention (PCI); (2) Participants lacking complete clinical data or images with insufficient quality for analysis; (3) Patients with severe hepatic or renal impairment, haematological disorders, immune system dysfunction, or malignant neoplasms. A total of 381 CHD patients were included. According to the 2020 European Society of Cardiology (ESC) guidelines, severe coronary stenosis was defined as 70%–99% luminal narrowing in major epicardial coronary arteries, >50% stenosis or complete occlusion of the left main coronary artery, or 100% vessel occlusion at the ICA [13]. Patients who did not meet the criteria for severe stenosis were classified as being in a mild-to-moderate group (Fig. 1).

2.2 Clinical Data

We have collected the first set of clinical data from electronic medical records. The data included the sex and age of the people. Laboratory measurements have been conducted as well, including low-density lipoprotein (LDL), high-density lipoprotein (HDL), triglycerides (TG), total cholesterol (TC), and fasting blood glucose (FBG). Record any past hypertension or diabetes also. Generally speaking, the above data are used to build an all-encompassing clinical risk assessment system for cardiovascular disease. Then a TyG index was calculated. It uses the formula ln[TG (mg/dL) × FBG (mg/dL)/2]; ln is the natural logarithm function in the above formula.

2.3 Ultrasound Imaging

All the patients were carotid ultrasound candidates. The examination was performed within 24 hours before their ICA. Philips EPIQ CVs colour Doppler ultrasound systems were used for all scans. An L12-3 linear array probe was connected to the machine. The range of frequencies for this probe is 3–12 MHz. The patient was lying down during the scan. They were told not to speak. Extend the neck slightly at the beginning. Turn the head to the side away from the artery you want to observe, which can help create the same view more easily. All the examination protocols for carotid imaging were the same. Adjust the parameters of a few machines. Gain, depth, and focus are the parameters listed above. To achieve good picture quality, optimise it has been carried out. If there were several carotid plaques, the one with the highest severity was selected for examination. The image plane has also been normalised. We used the view that showed the longest axis of the selected carotid plaque. All exported digital imaging and communications in medicine (DICOM) images were preprocessed with a set of preprocessing routines before feature extraction. The usual process had many steps. Normalisation of intensity is used to reduce the contrast difference in the picture;

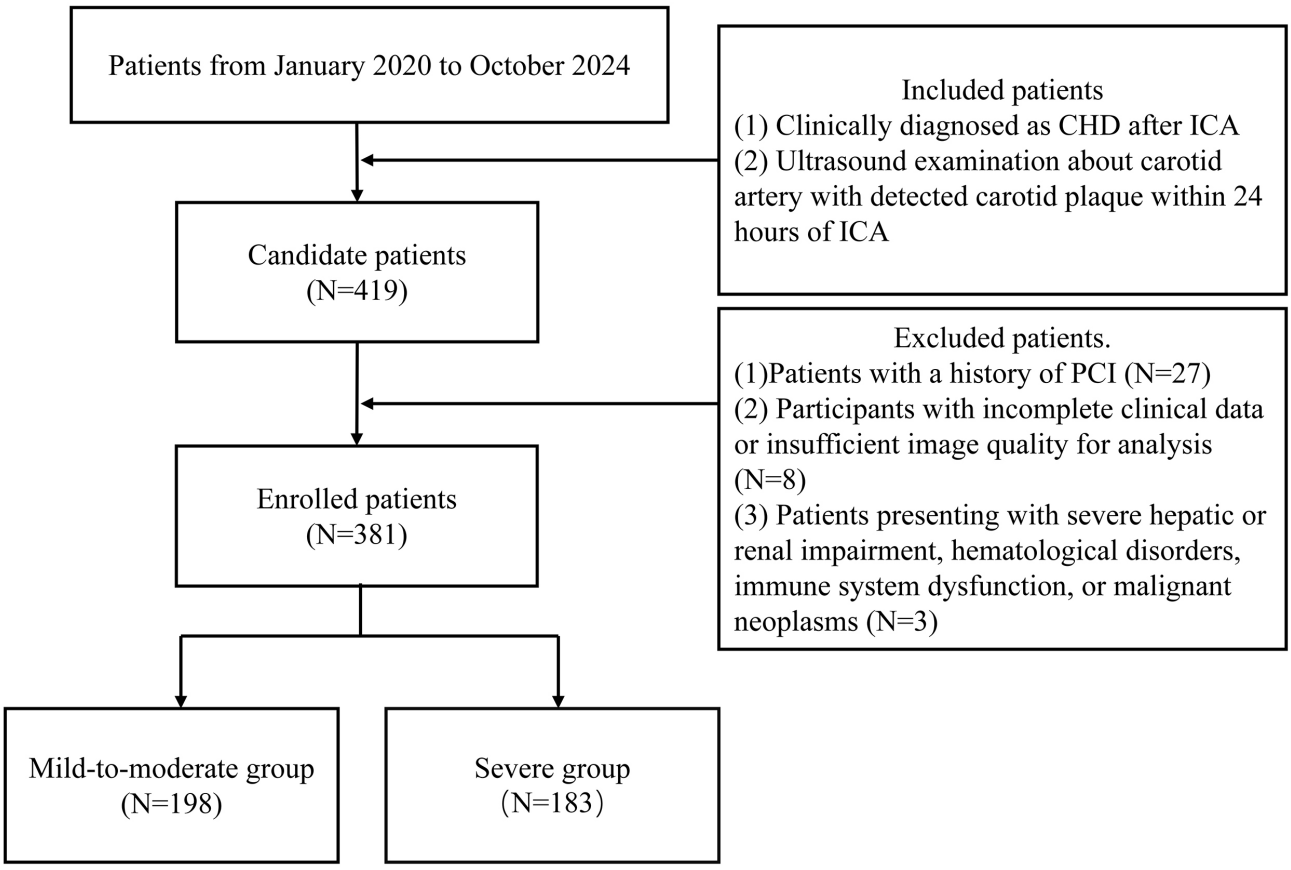

Fig. 1. Patient selection flowchart. CHD, coronary heart disease; ICA, invasive coronary angiography; PCI, percutaneous coronary intervention.

then, grayscale discretisation is applied to quantify the intensity range, and finally, a speckle-noise reduction filter is used to improve the uniformity of the image without losing structural features. A single experienced sonograp her (Sonographer A) carried out all the ultrasound examinations. To reduce the effect of observer bias, Sonographer A was unaware of any clinical data on the patients. It is a method of blinding.

2.4 Plaque Segmentation

DICOM images were imported into the Darwin Re search Platform (http://premium.darwin.yizhun-ai.com). Standard preprocessing was performed in this platform. The second skilled sonographer (Sonographer B) manually contoured the region of interest (ROI). This operator was also blinded to patient clinical data. The goal was to draw the boundaries of carotid plaques. To evaluate the reproducibility of the manual segmentation process and the stability of the derived radiomics features, inter- and intra-observer agreement were calculated. A small number of images were selected for independent segmentation by Sonographer B and a third, experienced sonographer (Sonographer C), and then inter-observer reliability was calculated. Sonographer B also repeated the segmentation of the same image set after a two-week period to evaluate intra-observer reliability. Consistency of segmentation was measured by the intraclass correlation coefficient (ICC) for continuous radiomics features, and an ICC value >0.75 was considered to indicate good or acceptable reproducibility; thus, the stability of the manual contouring step in the radiomics pipeline was assured. The results showed that the intra-observer ICC was 0.83 (95% confidence interval [CI]: 0.77–0.89) and the inter-observer ICC was 0.78 (95% CI: 0.75–0.84); both met the set criteria, and thus the stability of the manual contouring step in the radiomics pipeline was confirmed.

2.5 Feature Extraction and Model Construction

ROI segmentation was performed to extract a total of 1125 radiomics features per lesion automatically by the specified platform. The entire dataset was randomly split into a training set and a test set at an 8:2 ratio in the study, and to avoid scale differences and data leakage, feature standardisation was performed based only on the training set. To be specific, the mean and standard deviation of each feature were calculated from the training data, and then these features were standardised to have a mean of 0 and a standard deviation of 1. The standardised parameters

were then applied to process the independent test set. Feature selection is a two-step method that is applied only to the training data. First, recursive feature elimination (RFE) was used. This way, we will train a base classifier on the training set iteratively and then remove the least important feature in each cycle. The RFE algorithm itself selected the optimal number of features by considering cross-validation performance on the training set. A filt er-based approach was used on the remaining 33 features at this time. The analysis of variance (ANOVA) F-value for each one was calculated to determine whether it is linearly related to the outcome label. Finally, the 17 features with the largest F-values, that could distinguish the classes best, were chosen for the final model.

The three models built in this paper are for predicting the extent of coronary artery narrowing. Model A is a clinical model that uses only demographic and metabolic variables. Model B is a radiomics model derived from features extracted from ultrasound images. Model C is a combined multimodal model that includes both clinical variables and radiomics. All the models are logistic regressions. The model gave a specific weight coefficient (β_i) to each feature in training. The above weights are used to calculate the individual radiomics score (Rad score) of a patient via the formula: Rad score = $\beta_0 + \Sigma(\beta_i \times \text{Feature}_i)$. Model C was built by taking both the original clinical variables and the new Rad score from Model B as inputs for another logistic regression classifier. The second is that an independent test set will be reserved. It did not participate in feature processing, selection, or model training; only at the end would its results be displayed. The seven typical indices that will be used for model evaluation are as follows: Area under the curve (AUC), accuracy, sensitivity, specificity, positive predictive value (PPV), negative predictive value (NPV), and F1 score. A threshold of 0.5 is set for the probability output of the model in classification. Calibration curves and decision curve analysis (DCA) were employed in the subsequent tests of model reliability to determine how to apply it in practice. Finally, to understand why the model made certain predictions, we used SHapley Additive exPlanations (SHAP) to analyse it. Summary plots were used to show the results of the above feature importance analysis.

2.6 Statistical Analysis

All of the above statistics were analysed in IBM SPSS Statistics 24.0 (IBM Corp., Armonk, NY, USA). Shapiro–Wilk test was employed to check whether the continuous variables were normally distributed. Mean ± standard deviation (SD) was used for normally distributed continuous data, and the median (interquartile range, IQR) was employed for non-normally distributed continuous data. Categorical variables are shown as numbers and percentages. The differences in normally distributed continuous variables among the groups were tested by an independent-samples *t*-test, and the Mann–Whitney U test was used for non-normally distributed continuous variables. A chi-squared test was performed on the categorical variables. Variables with a p value < 0.05 in the univariate logistic regression analysis were subsequently included in the multivariate logistic regression model to determine independent risk factors. Before building the model, the variance inflation factor (VIF) of the proposed predictors to test for multicollinearity was calculated, and a threshold of 10 was set for severe multicollinearity. The results are presented as odds ratio (OR), 95% CI, β coefficient, standard error (SE), and *p*-value. A DeLong test is used to compare the statistical differences of AUC for multiple models. A two-tailed $p < 0.05$ was taken as the threshold.

3. Results

3.1 Comparison of Baseline Clinical Data

Tables 1,2 show the characteristics of the baseline patients. The two groups of patients in this study were 198 (52.0%) with mild-to-moderate coronary stenosis and 183 (48.0%) with severe coronary stenosis. When the patients were divided into groups according to the severity of stenosis, the severe group had a significantly higher level of TG ($p < 0.001$), FBG ($p < 0.001$), and TyG index ($p < 0.001$). They also had much lower HDL values ($p = 0.003$) compared to those in the mild-to-moderate group. The severe group was also significantly more likely to be male ($p = 0.013$) and had a higher incidence of hypertension ($p < 0.001$) and diabetes ($p = 0.006$). There were no significant differences between the training and test sets for any of the baseline clinical variables (all $p > 0.05$). Thus, the two datasets are in good agreement and have been balanced after the split. Therefore, the two need to be jointly used in model construction and verification.

3.2 Selection of Clinical Features

The VIF analysis indicated collinearity between TG and the TyG index. Since the TyG index is a metabolic indicator calculated from both TG and FBG, TG was excluded in the multivariate analysis, while the TyG index was retained to improve model stability and estimation accuracy. Univariate and multiple logistic regression analysis (Table 3) identified the following three clinical factors that are correlated with the extent of coronary artery stenosis: Sex ($p = 0.025$), TyG index ($p < 0.001$), and hypertension status ($p = 0.012$).

3.3 Radiomics Features

Starting with an initial pool of 1125 features, 17 representative radiomics features were finally selected for predicting the severity of severe coronary lesions. The Rad score of each patient was computed by the following weighted linear combination:

Table 1. Clinical characteristics of all patients.

Clinical features	Mild-**to**-moderate group (198)	Severe group (183)	χ^2/Z/*t*	*p*
Age (years)	67.00 (60.0, 73.0)	68.00 (62.0, 73.0)	–0.993	0.321
Sex			6.212	0.013
Male	120 (60.6%)	133 (72.7%)		
Female	78 (39.4%)	50 (27.3%)		
LDL (mmol/L)	2.30 (1.81, 2.89)	2.44 (1.81, 3.12)	–1.713	0.087
HDL (mmol/L)	1.25 (1.09, 1.46)	1.17 (1.00, 1.37)	–3.016	0.003
TC (mmol/L)	3.98 (3.41, 4.62)	4.08 (3.41, 4.91)	–1.395	0.163
TG (mmol/L)	1.06 (0.77, 1.39)	1.43 (1.05, 1.90)	–6.508	<0.001
FBG (mmol/L)	5.03 (4.62, 5.59)	5.61 (4.91, 6.49)	–5.347	<0.001
TyG index	8.37 ± 0.46	8.77 ± 0.50	–8.174	<0.001
Hypertension status			12.843	<0.001
Yes	96 (48.5%)	122 (66.7%)		
No	102 (51.5%)	61 (33.3%)		
Diabetes status			7.445	0.006
Yes	27 (13.6%)	45 (24.6%)		
No	171 (86.4%)	138 (75.4%)		

LDL, low-density lipoprotein; HDL, high-density lipoprotein; TC, total cholesterol; TG, triglycerides; FBG, fasting blood glucose; TyG, triglyceride-glucose.

Table 2. Comparison of clinical characteristics between the training set and the test set.

Clinical features	Training set (304)	Test set (77)	χ^2/Z/*t*	*p*
Age (years)	67.00 (60.0, 73.0)	67.00 (62.0, 72.0)	–0.004	0.965
Sex			0.001	0.972
Male	202 (66.4%)	51 (66.2%)		
Female	102 (33.6%)	26 (33.8%)		
LDL (mmol/L)	2.40 (1.83, 3.01)	2.26 (1.74, 2.95)	–0.754	0.450
HDL (mmol/L)	1.22 (1.05, 1.41)	1.22 (1.06, 1.44)	–0.587	0.557
TC (mmol/L)	4.06 (3.43, 4.78)	4.02 (3.41, 4.66)	–0.639	0.524
TG (mmol/L)	1.19 (0.90, 1.61)	1.26 (0.91, 1.66)	–0.166	0.868
FBG (mmol/L)	5.28 (4.78, 6.07)	5.06 (4.59, 6.21)	–1.605	0.108
TyG index	8.56 ± 0.51	8.54 ± 0.55	–0.373	0.709
Hypertension status			0.252	0.616
Yes	172 (56.6%)	46 (59.7%)		
No	132 (43.4%)	31 (40.3%)		
Diabetes status			0.021	0.884
Yes	57 (18.8%)	15 (19.5%)		
No	247 (81.2%)	62 (80.5%)		
Severity			0	1.000
Mild-to-moderate	158 (52.0%)	40 (52.0%)		
Severe	146 (48.0%)	37 (48.0%)		

Radscore=+0.525×original_shape2D_MaximumDiameter
+0.475×exponential_glrlm_GrayLevelNonUniformity
–0.467 × wavelet-HL_glcm_InverseVariance
–0.396 × wavelet-HL_glcm_MaximumProbability
+0.337×wavelet-LH_gldm_LargeDependenceEmphasis
–0.286 × wavelet-LH_glrlm_RunPercentage
+0.257 × wavelet-LH_glcm_MaximumProbability
–0.251 × square_glrlm_GrayLevelNonUniformity
–0.232 × original_shape2D_Perimeter
–0.231 × lbp-2D_glrlm_GrayLevelNonUniformity
--0.206×wavelet-HL_gldm_LargeDependenceEmphasis
+0.196 × gradient_glrlm_GrayLevelNonUniformity
+0.160 × wavelet-LH_glcm_JointEnergy
+0.135 × wavelet-HL_glrlm_RunPercentage
–0.067 × lbp-2D_firstorder_Mean
–0.059 × original_shape2D_MajorAxisLength
+0.005 × lbp-2D_firstorder_RootMeanSquared-0.080

Table 3. Candidate clinical predictors after logistic regression analysis.

Clinical features	Univariate analysis			Multivariate analysis		
	OR (95% CI)	β (SE)	*p*	OR (95% CI)	β (SE)	*p*
Age	1.01 (0.99, 1.03)	0.01 (0.01)	0.413			
Sex	1.73 (1.12, 2.67)	0.55 (0.22)	0.013	1.80 (1.08, 3.00)	0.59 (0.26)	0.025
LDL	1.28 (1.00, 1.63)	0.25 (0.12)	0.050			
HDL	0.31 (0.15, 0.63)	–1.17 (0.38)	0.001	0.69 (0.29, 1.65)	–0.37 (0.45)	0.403
TC	1.22 (0.99, 1.50)	0.20 (0.10)	0.067			
TG	3.12 (2.08, 4.67)	1.14 (0.21)	<0.001			
FBG	1.84 (1.47, 2.29)	0.61 (0.11)	<0.001	1.20 (0.98, 1.46)	0.18 (0.10)	0.071
TyG index	5.84 (3.57, 9.57)	1.76 (0.25)	<0.001	3.82 (2.13, 6.84)	1.34 (0.30)	<0.001
Hypertension status	2.13 (1.40, 3.22)	0.76 (0.21)	<0.001	1.81 (1.14, 2.87)	0.59 (0.24)	0.012
Diabetes status	2.07 (1.22, 3.50)	0.73 (0.27)	0.007	0.66 (0.32, 1.34)	–0.42 (0.37)	0.245

OR, odds ratio; 95% CI, 95% confidence interval; SE, standard error.

Variable coding: Sex was coded as 1 for male; hypertension status was coded as 1 for the presence of hypertension; diabetes status was coded as 1 for the presence of diabetes.

The three radiomics features that showed a stronger a ssociation in themodel were original_shape2D_Maximum Diameter,exponential_glrlm_GrayLevelNonUniformity, a ndwavelet-HL_glcm_InverseVariance. Original_shape2D _MaximumDiameter isa shape-based descriptor of the larg est diameter of the plaque. A largermaximum diameter of t he plaque is associated with an increased risk ofsevere lesi ons, and thus has a positive regression coefficient.

Exponential_glrlm_GrayLevelNonUniformity describes the texture heterogeneity of the plaque. Higher values of this feature indicates that an increase in internal echo heterogeneity is associated with a higher risk score.

Wavelet-HL_glcm_InverseVariance is another text ure feature of local uniformity. The negative coeff icient indicates that a more even texture of plaque is associated with a reduced risk.

3.4 Model Construction and Evaluation

Three different prediction models were built. Model A (clinical model) includes sex, TyG index, and hypertension status. Model B (radiomics model) only used the Rad score. Model C (combined model) combined both clinical and radiomics features. The diagnostic performance of the three models is shown in Fig. 2. The AUC of Model A on the training set was 0.728 (95% CI: 0.671–0.784). The test set was 0.663 (95% CI: 0.539–0.787). Sensitivity and specificity were 0.772/0.667 and 0.750/0.550. Accuracy is 0.717/0.645. PPV is 0.679/0.600. NPV is 0.763/0.710. F1 score = 0.723/0.667, and Model B (Rad score alone) has an AUC of 0.673 (95% CI: 0.613–0.734) on the training set. In the test set, it was 0.686 (95% CI: 0.567–0.806). The sensitivity and specificity are 0.593/0.704 and 0.611/0.650, respectively. Accuracy is 0.651/0.632. PPV = 0.647/0.611. NPV is 0.655/0.650. F1 score: 0.619/0.611; Model C performed the best. The AUC of the training set was 0.823 (95% CI: 0.777–0.870). The AUC of the test set was 0.730 (95% CI: 0.616–0.844). Sensitivity and specificity are 0.876/0.610 and 0.694/0.725, respectively. Accuracy is 0.737/0.711. PPV was 0.672/0.694. NPV is 0.843/0.725. The F1 score is 0.760/0.694.

DeLong test was used to compare the AUC of the models. Model C had a relatively high discrimination performance in the training set compared to Model A (p = 0.008) and Model B ($p < 0.001$). Model C also performed better than each single-modality model in the test set for predicting coronary lesion severity (p = 0.032 vs. Model A; p = 0.041 vs. Model B). A calibration curve was used to compare the predicted probability of coronary artery stenosis from Model C with the actual incidence of coronary artery stenosis (Fig. 3). The fit to the training data is reasonably good. A good calibration result was also obtained in the test set. DCA was performed to assess the clinical net benefit of the combined model (Fig. 4). Analysis showed that at various threshold probabilities, Model C had demonstrated a better clinical net benefit than both the “treat-all” and “treat-none” approaches.

Two types of plots based on SHAP have been generated for interpretability: A force plot (Fig. 5) showing the reasons for individual predictions, and a beeswarm plot (Fig. 6) displaying the global distribution of all feature values. The force plot displays the SHAP values of each feature for an individual prediction. Beeswarm plots were used to show the patterns of feature importance in the whole cohort. Therefore, it was found that the Rad score was a good indicator of high-risk coronary heart disease. TyG index followed, and a larger value of both indicators led to an increased risk. As shown in the force plot, hypertension, a high TyG index, and an elevated Rad score were associated with an increased risk; however, for the representative individual case, being female reduced the risk.

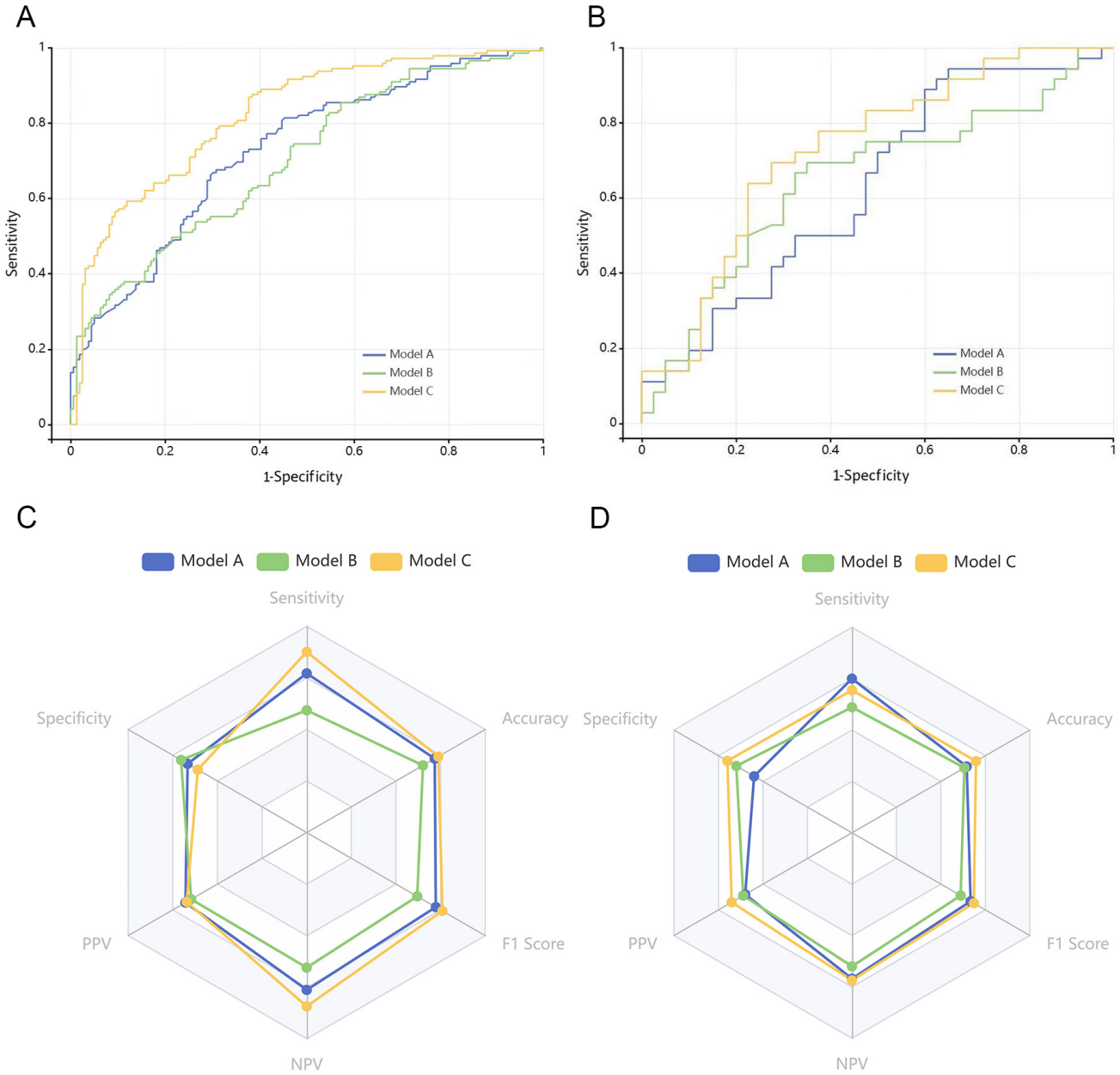

Fig. 2. Diagnostic performance of the three prediction models in the training and testsets. (A) ROC curves of the three models in the training set. (B) ROC curves of the three models in the test set. (C) Radar chart of the diagnostic performance of the three models in the training set. (D) Radar chart of the diagnostic performance of the three models in the test set. ROC, receiver operating characteristic; PPV, positive predictive value; NPV, negative predictive value. Model A, clinical model; Model B, radiomics model; Model C, combined model.

4. Discussion

Determine the severity of damage to the coronary lesions and improve the diagnostic and treatment plans for CHD. Personalized treatment and the prediction of disease evolution are enabled. Although invasive coronary angiography (ICA) anterior oblique coronary angiography has relatively good accuracy, it is still a common first step in the evaluation to perform conventional coronary angiography. However, due to procedural risks and high costs, it has not been implemented. Therefore, they have been used sparingly. As medical images have developed in recent years, so too have new methods for extracting information from them. The above method is suitable for the extraction of high-throughput quantitative features from images. Algorithms of artificial intelligence can also be employed to conduct fine-grained studies of lesion biology. Radiomics is a non-invasive method that can now be used to assess the severity of coronary lesions. It is not an invasive method. We have combined radiomics features of carotid ultrasound and clinical data in a new way here.

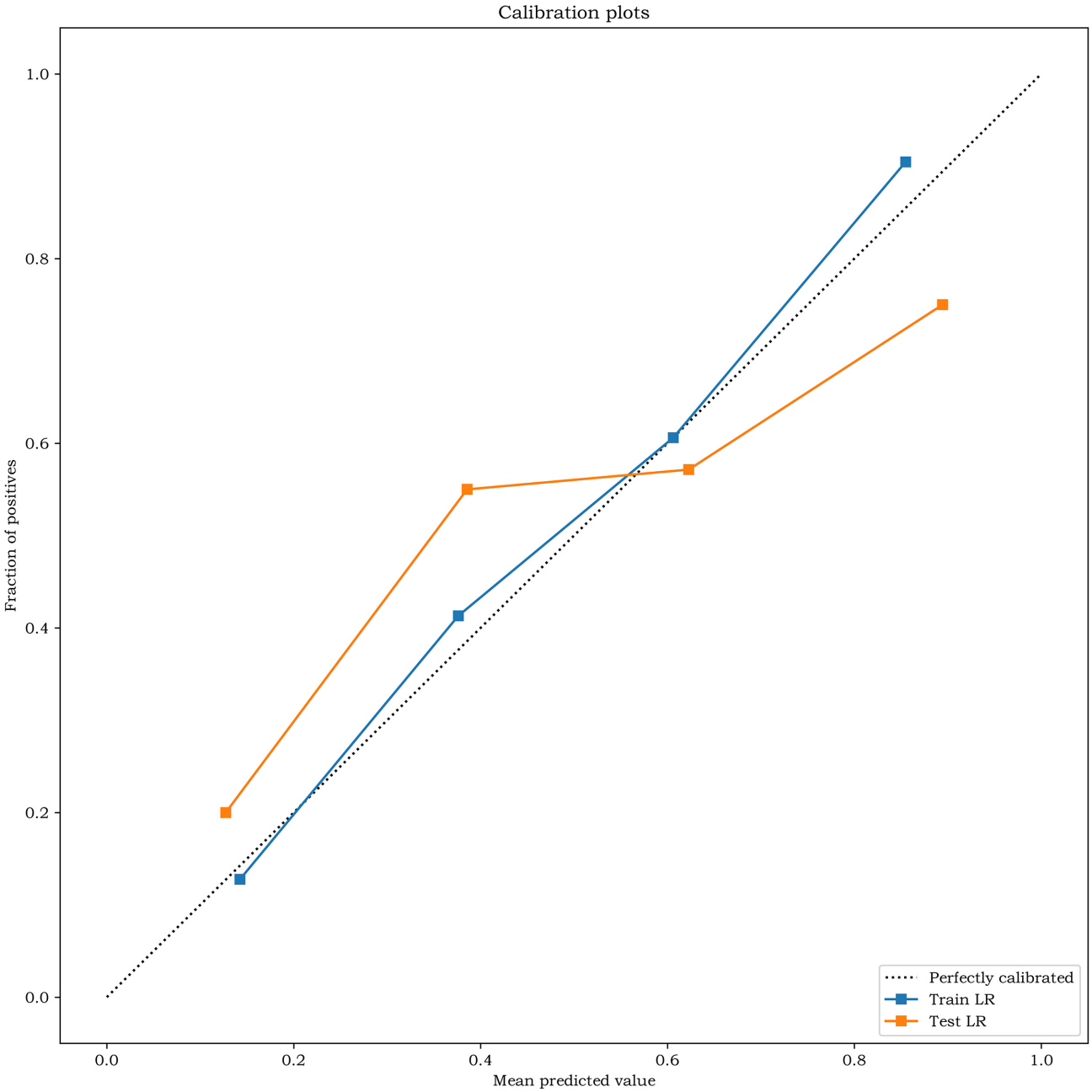

Fig. 3. Calibration curves of Model C in the training and test sets. LR, logistic regression.

The above integrations formed the basis of a prediction model. Our model is more precise in grading and can be applied clinically compared with single-modality methods.

Many other groups have been studying the radiomics of coronary artery lesions before this study. At the same time, other related studies have explored the identification of atherosclerotic plaques [14], the assessment of coronary inflammation [15], and the prediction of coronary calcification and stenosis [16]. Based on this background, our research has discovered that radiomics features in carotid ultrasound images also possess good predictive capabilities for the severity of coronary artery lesions. After feature selection, the 17 best-performing ultrasonic radiomics features were selected as the indicators of coronary severity. Then, we built a machine learning model for coronary lesion grading. This model combined the ultrasonic radiomics features with clinical risk factors, and the combined model (Model C) reached an AUC of 0.823 (95% CI: 0.777–0.870) in the training set and 0.730 (95% CI: 0.616–0.844) in the independent test set. It outperformed the model that used only traditional clinical indices (Model A) and the unimodal radiomics feature model (Model B) significantly. A reasonable calibration curve and a positive net benefit in DCA also show that the model is reliable and applicable to the clinic; this result is in line with other studies of cardiovascular radiomics [17].

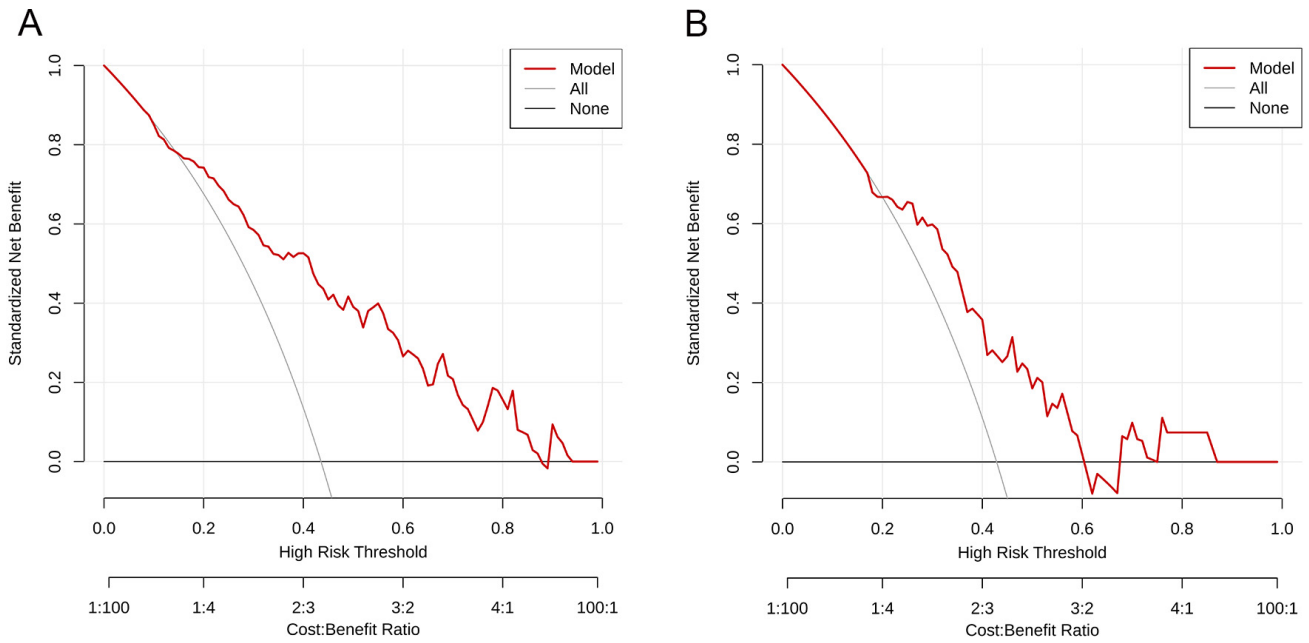

Fig. 4. DCA of Model C in the training and test sets. (A) DCA of Model C in the training set. (B) DCA of Model C in the test set. DCA, decision curve analysis. The "Model" curve (solid line) shows the net benefit when clinical decisions are guided by the combined prediction model; the "All" curve (dashed line) represents the net benefit assuming all patients receive intervention (treat-all strategy); and the "None" curve (horizontal line at y=0) represents the net benefit assuming no patients receive intervention (treat-none strategy), serving as the baseline reference.

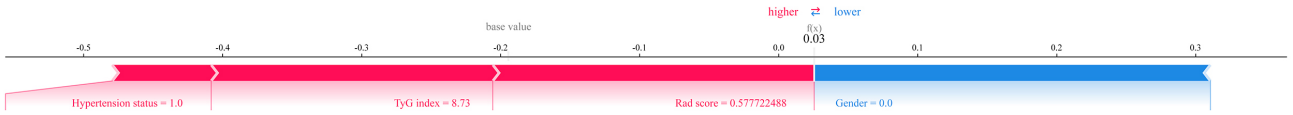

Fig. 5. Force plot visualisation: hypertensive female with severe coronary stenosis (severe group). Variable coding: Sex was coded as 1 for male, and hypertension status was coded as 1 for having hypertension. Rad score, radiomics score.

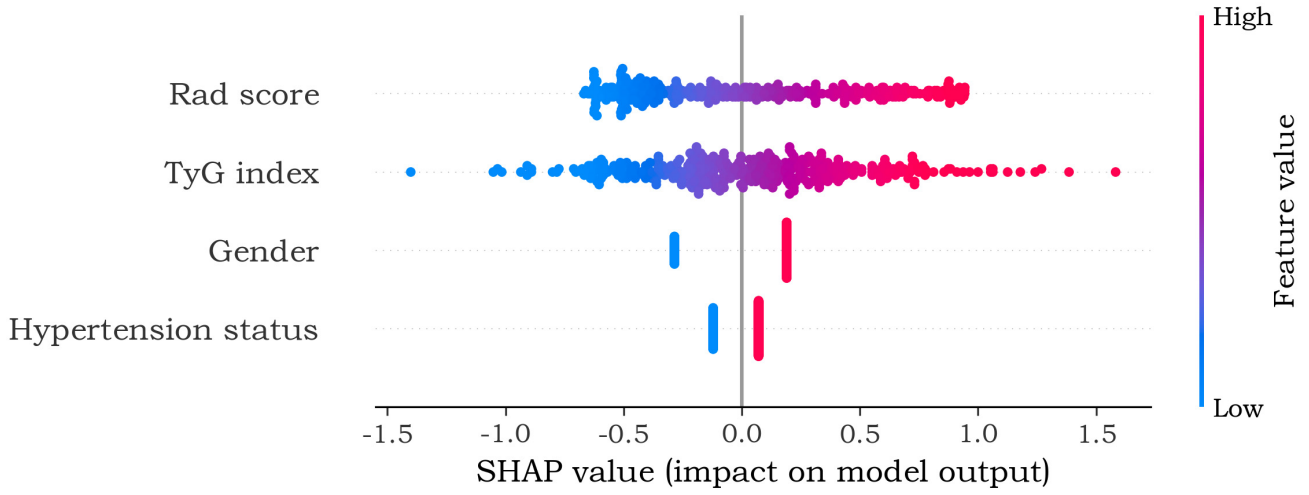

Fig. 6. Beeswarm plot of feature distribution and clinical effect. Variable coding: Sex was coded as 1 for male, and the presence of hypertension was coded as 1. SHAP, SHapley Additive exPlanations.

Therefore, multimodal data fusion needs to be employed to improve the accuracy of non-invasive coronary assessment. Merge systemic metabolic indicators (TyG index) and local vascular imaging characteristics (carotid

radiomics) to overcome the limitations of single-modality approaches in our model.

SHAP plots are used to show the results and reasons for the model. The above graphs show the effects of the features on the predicted value. Thus, the model's decision-making process has been made more transparent and the reasons for the drop in accuracy identified. The previous studies have shown that it is feasible to use this model [18,19]; to make the prediction of coronary lesion severity more intuitive, a beeswarm plot for model visualisation has been developed. The beeswarm plot more intuitively illustrates how the distribution of feature values is associated with changes in lesion severity, thereby facilitating clinical interpretation and visualising the results of the SHAP-based feature attribution analysis. Thus, it quantifies the predictive power of various attributes for a particular person. The resulting force plots are customised visualisations of feature importance. The data will help the doctor understand why a patient has a high or low risk. They can also explore the interaction among features [20], and the interpretability framework we established has a dual purpose of clinical translation. First, it is possible to show the prediction logic of a complicated model in a simple-to-use visual form. Second, it is possible to measure the added benefits of biomarkers in disease progression. The open channel can help the public trust radiomics more easily and provide a stable support system for implementing radiomics-based technologies in the clinic.

Some previous studies have identified associations among hypertension, sex, and the degree of coronary artery disease [21,22,23]. Our research provides the above support. Hypertension (OR: 1.81, 95% CI: 1.14–2.87) and male sex (OR: 1.80, 95% CI: 1.08–3.00) were identified as independent risk factors for severe coronary lesions in patients with CHD, and the new function of the TyG index as an independent predictor of coronary severity was also confirmed. Wang and others have found that a higher TyG index was associated with an increased risk of multi-vessel coronary artery disease. They pointed out its application in measuring CAD severity by IR estimation [24]. TyG index changes in IR and glycolipid metabolic diseases are not pronounced. Quantify the combined impact of triglycerides and glucose metabolism to do so [25]. Pathways are relatively numerous. First, IR causes endothelial dysfunction by reducing the activity of endothelial nitric oxide synthase (eNOS). This will form a plaque [26]. Second, hypertriglyceridemia promotes the deposition of triglyceride-rich lipoproteins (TRLs). It will also activate the nuclear factor kappa B (NF-κB) pathway and cause inflammation of the vascular wall [27]. Thirdly, impaired glucose metabolism will be prone to generating harmful end products of glycation. It will hasten the development of coronary calcification [28]. The TyG index is a relatively simple-to-use index. The diagnostic thresholds have not been normalised yet. Therefore, the clinical interpretation should be in conjunction with other metabolic indicators [29], and in this study, HDL, TG, FBG and diabetes status were all statistically significant in univariate logistic regression. They were not statistically significant in the multivariate analysis. This does not match the above data [30,31,32,33]. We believe that this is probably due to the daily consumption of cholesterol-reducing and blood-sugar-lowering drugs by the members of our group. The cross-sectional design of this retrospective study may also be added. In the future, we will look at the connection among the various lipid indices and FBG with coronary lesions prospectively.

The following are some limitations of this study: First, the data were only collected at one centre. The past design may be less applicable to all groups of people in the wide population. A forward-looking multi-centre study for external validation will be conducted. Second, as it is a retrospective study, it cannot fully rule out confounding factors caused by changes in patients' medication. Patient inclusion was not randomised, and the third was a binary system for coronary lesion severity. This way is too general. The next research will be a quantitative one, and we will use the SYNTAX (synergy between percutaneous coronary intervention with TAXUS and cardiac surgery) score and the Gensini score. They will enable more refined divisions of the complexity and severity of the lesions. They can also perform fine-grained risk analysis in a hospital.

5. Conclusion

In this study, we developed a non-invasive model combining the TyG index and carotid plaque radiomics to predict severe coronary stenosis in CHD patients. The combined model outperformed single-modality approaches, indicating that systemic metabolic dysfunction and local plaque heterogeneity provide complementary information on lesion severity. This integrated tool offers a practical strategy for early risk stratification, potentially reducing unnecessary invasive coronary angiography and supporting personalized treatment decisions. Future prospective, multicenter studies with quantitative angiographic scoring are warranted to validate its clinical utility and prognostic value.

Key Points

- This paper intends to build a non-invasive multimodal model that integrates TyG index and carotid plaque ultrasound radiomics features to evaluate the severity of coronary artery lesions and overcome the deficiencies of ICA.
- Multivariate analysis was performed on this retrospective single-centre study of coronary heart disease (CHD) patients to identify clinical predictors, and a

radiomics score was established using the two-step strategy for feature selection in the training set.

• The combined model integrates clinical predictors and a radiomics score, and this model performs better in terms of discrimination than either model individually; both the training and test sets show an increase in AUC.

• The results show that the combined model may serve as an early indicator of pre-procedure risks non-invasively; however, due to the study design limitations, further prospective multi-centre validation is still needed.

Availability of Data and Materials

The datasets generated and analysed during the current study are not publicly available due to patient privacy and scales copyright but are available from the corresponding author on reasonable request.

Author Contributions

HTH and CZ designed the study. RYZ, AYZ, WSH, XYL and HTH performed the study. DS and HTH analysed and interpreted the data. HTH drafted the first version of the manuscript. All authors participated in the critical revision of the manuscript for important intellectual content. All authors have read and approved the final manuscript. All authors have fully participated in the work and agreed to be accountable for all aspects of the work, ensuring that any questions related to the accuracy or integrity of the research content are appropriately investigated and resolved.

Ethics Approval and Consent to Participate

This study was conducted in accordance with the principles of the Declaration of Helsinki. As a retrospective analysis of anonymised clinical and imaging data, it was reviewed and approved by the Ethics Committee of The First College of Clinical Medical Science, China Three Gorges University and Yichang Central People's Hospital (Ethics Approval No.: 2025-191-01). Given the retrospective nature of the study and the use of anonymised data, the requirement for informed consent was waived by the aforementioned ethics committee. All patient data were handled with strict confidentiality.

Acknowledgment

The design of the experimental choices was based on patients with coronary heart disease. We acknowledge the contribution of all patients and their caregivers. Besides, ultrasound teachers also provided a lot of help and expressed their thoughts and views, which were considered and included in the project implementation.

Funding

This research was supported by the Natural Science Foundation of Hubei Province (No. 2025AFD260).

Conflicts of Interest

The authors declare no conflicts of interest.

Declaration of AI and AI-Assisted Technologies in the Writing Process

We used the Darwin Research Platform (http://premium.darwin.yizhun-ai.com). It is a tool for AI-aided medical image analysis. It was employed for standardized preprocessing and high-throughput extraction of radiomics features. It also provided SHAP visualisations, and all AI output was manually verified. These included feature values and segmentation parameters. Two scholars conducted the above research. They have good knowledge of cardiovascular imaging and radiomics. They confirmed the data, removed potential bias, and ensured accuracy. We did not use generative AI tools. We did not use a large language model. No AI-written text was used at any time. This covers study design, data collection, and analysis. It also covers interpretation, drafting, and revision. All text and reasoning in this manuscript came from the authors. The authors take full responsibility. They stand by the scientific validity and data integrity.

References

[1] Bergmark BA, Mathenge N, Merlini PA, Lawrence-Wright MB, Giugliano RP. Acute coronary syndromes. Lancet (London, England). 2022; 399: 1347–1358. https://doi.org/10.1016/S0140-6736(21)02391-6

[2] Florek K, Kübler M, Górka M, Kübler P. New Modifiable Risk Factors Influencing Coronary Artery Disease Severity. International Journal of Molecular Sciences. 2024; 25: 7766. https://doi.org/10.3390/ijms25147766

[3] Martin SS, Aday AW, Allen NB, Almarzooq ZI, Anderson CAM, Arora P, et al. 2025 Heart Disease and Stroke Statistics: A Report of US and Global Data From the American Heart Association. Circulation. 2025; 151: e41–e660. https://doi.org/10.1161/CIR.0000000000001303

[4] Bertolone DT, Gallinoro E, Esposito G, Paolisso P, Bermpeis K, De Colle C, et al. Contemporary Management of Stable Coronary Artery Disease. High Blood Pressure & Cardiovascular Prevention: the Official Journal of the Italian Society of Hypertension. 2022; 29: 207–219. https://doi.org/10.1007/s40292-021-00497-z

[5] Mézquita AJV, Biavati F, Falk V, Alkadhi H, Hajhosseiny R, Maurovich-Horvat P, et al. Clinical quantitative coronary artery stenosis and coronary atherosclerosis imaging: a Consensus Statement from the Quantitative Cardiovascular Imaging Study Group. Nature Reviews. Cardiology. 2023; 20: 696–714. https://doi.org/10.1038/s41569-023-00880-4

[6] Park HM, Lee HS, Lee YJ, Lee JH. The triglyceride-glucose index is a more powerful surrogate marker for predicting the prevalence and incidence of type 2 diabetes mellitus than the homeostatic model assessment of insulin resistance. Diabetes

Research and Clinical Practice. 2021; 180: 109042. https://doi.org/10.1016/j.diabres.2021.109042

[7] Li C, Qi Q, Li W, Zhang X, Li L, Deng J, et al. Triglyceride-Glucose Index Predicts Major Adverse Cardiovascular and Cerebrovascular Events in Non-Diabetic Individuals. Balkan Medical Journal. 2025; 42: 339–346. https://doi.org/10.4274/balkanmedj.galenos.2025.2025-2-109

[8] Lopez-Jaramillo P, Gomez-Arbelaez D, Martinez-Bello D, Abat MEM, Alhabib KF, Avezum Á, et al. Association of the triglyceride glucose index as a measure of insulin resistance with mortality and cardiovascular disease in populations from five continents (PURE study): a prospective cohort study. The Lancet. Healthy Longevity. 2023; 4: e23–e33. https://doi.org/10.1016/S2666-7568(22)00247-1

[9] Liang S, Wang C, Zhang J, Liu Z, Bai Y, Chen Z, et al. Triglyceride-glucose index and coronary artery disease: a systematic review and meta-analysis of risk, severity, and prognosis. Cardiovascular Diabetology. 2023; 22: 170. https://doi.org/10.1186/s12933-023-01906-4

[10] Bytyçi I, Shenouda R, Wester P, Henein MY. Carotid Atherosclerosis in Predicting Coronary Artery Disease: A Systematic Review and Meta-Analysis. Arteriosclerosis, Thrombosis, and Vascular Biology. 2021; 41: e224–e237. https://doi.org/10.1161/ATVBAHA.120.315747

[11] Liu D, Du C, Shao W, Ma G. Diagnostic Role of Carotid Intima-Media Thickness for Coronary Artery Disease: A Meta-Analysis. BioMed Research International. 2020; 2020: 9879463. https://doi.org/10.1155/2020/9879463

[12] Fuster V, García-Álvarez A, Devesa A, Mass V, Owen R, Quesada A, et al. Influence of Subclinical Atherosclerosis Burden and Progression on Mortality. Journal of the American College of Cardiology. 2024; 84: 1391–1403. https://doi.org/10.1016/j.jacc.2024.06.045

[13] Collet JP, Thiele H, Barbato E, Barthélémy O, Bauersachs J, Bhatt DL, et al. 2020 ESC Guidelines for the management of acute coronary syndromes in patients presenting without persistent ST-segment elevation. European Heart Journal. 2021; 42: 1289–1367. https://doi.org/10.1093/eurheartj/ehaa575

[14] Chen Q, Pan T, Wang YN, Schoepf UJ, Bidwell SL, Qiao H, et al. A Coronary CT Angiography Radiomics Model to Identify Vulnerable Plaque and Predict Cardiovascular Events. Radiology. 2023; 307: e221693. https://doi.org/10.1148/radiol.221693

[15] Shang J, Ma S, Guo Y, Yang L, Zhang Q, Xie F, et al. Prediction of acute coronary syndrome within 3 years using radiomics signature of pericoronary adipose tissue based on coronary computed tomography angiography. European Radiology. 2022; 32: 1256–1266. https://doi.org/10.1007/s00330-021-08109-z

[16] Homayounieh F, Yan P, Digumarthy SR, Kruger U, Wang G, Kalra MK. Prediction of Coronary Calcification and Stenosis: Role of Radiomics From Low-Dose CT. Academic Radiology. 2021; 28: 972–979. https://doi.org/10.1016/j.acra.2020.09.021

[17] Lambin P, Leijenaar RTH, Deist TM, Peerlings J, de Jong EEC, van Timmeren J, et al. Radiomics: the bridge between medical imaging and personalized medicine. Nature Reviews. Clinical Oncology. 2017; 14: 749–762. https://doi.org/10.1038/nrclinonc.2017.141

[18] Manikis GC, Ioannidis GS, Siakallis L, Nikiforaki K, Iv M, Vozlic D, et al. Multicenter DSC-MRI-Based Radiomics Predict IDH Mutation in Gliomas. Cancers. 2021; 13: 3965. https://doi.org/10.3390/cancers13163965

[19] Xie W, Shi R, Xiang J, Chen B, An DA, Zhou Y, et al. Machine Learning Using Clinical and Cardiac MRI Features to Predict Long-term Outcomes in Acute STEMI. Radiology. 2026; 318: e251490. https://doi.org/10.1148/radiol.251490

[20] Wang L, Wei C, Chen Y, Lu DS, Zhang HX, Yang M. Machine learning-based prediction model for 30-day readmission risk in elderly patients with type 2 diabetes mellitus and heart failure: a retrospective cohort study with SHAP interpretability analysis. Frontiers in Cardiovascular Medicine. 2026; 12: 1673159. https://doi.org/10.3389/fcvm.2025.1673159

[21] Ling Q, Dong X, Zhao X, Cai J. Sex Differences in Achieved Diastolic Blood Pressure and Cardiovascular Outcomes in Elderly Patients With Hypertension. JACC. Advances. 2025; 4: 101675. https://doi.org/10.1016/j.jacadv.2025.101675

[22] Puddu PE, Schiariti M, Torromeo C. Gender and Cardiovascular Mortality in Northern and Southern European Populations. Current Pharmaceutical Design. 2016; 22: 3893–3904. https://doi.org/10.2174/1381612822666160502153154

[23] Wang R, Gao W, Che X, Shen R, Dai C, Xia Y, et al. Clinical factors associated with severe coronary stenosis in patients undergoing cardiac surgery. BMC Cardiovascular Disorders. 2025; 25: 395. https://doi.org/10.1186/s12872-025-04835-0

[24] Wang X, Xu W, Song Q, Zhao Z, Meng X, Xia C, et al. Association between the triglyceride-glucose index and severity of coronary artery disease. Cardiovascular Diabetology. 2022; 21: 168. https://doi.org/10.1186/s12933-022-01606-5

[25] Tahapary DL, Pratisthita LB, Fitri NA, Marcella C, Wafa S, Kurniawan F, et al. Challenges in the diagnosis of insulin resistance: Focusing on the role of HOMA-IR and Tryglyceride/glucose index. Diabetes & Metabolic Syndrome. 2022; 16: 102581. https://doi.org/10.1016/j.dsx.2022.102581

[26] Bornfeldt KE, Tabas I. Insulin resistance, hyperglycemia, and atherosclerosis. Cell Metabolism. 2011; 14: 575–585. https://doi.org/10.1016/j.cmet.2011.07.015

[27] Nordestgaard BG. Triglyceride-Rich Lipoproteins and Atherosclerotic Cardiovascular Disease: New Insights From Epidemiology, Genetics, and Biology. Circulation Research. 2016; 118: 547–563. https://doi.org/10.1161/CIRCRESAHA.115.306249

[28] Brownlee M. The pathobiology of diabetic complications: a unifying mechanism. Diabetes. 2005; 54: 1615–1625. https://doi.org/10.2337/diabetes.54.6.1615

[29] Perticone M, Shehaj E, Suraci E, Andreozzi F, Perticone F. Individuation of a cut-off value of triglyceride-glucose index for incident diabetes mellitus in patients with essential hypertension. Internal and Emergency Medicine. 2025; 20: 423–429. https://doi.org/10.1007/s11739-024-03803-4

[30] Pérez-Méndez Ó, Pacheco HG, Martínez-Sánchez C, Franco M. HDL-cholesterol in coronary artery disease risk: function or structure? Clinica Chimica Acta; International Journal of Clinical Chemistry. 2014; 429: 111–122. https://doi.org/10.1016/j.cca.2013.12.001

[31] Asakura K, Minami Y, Kinoshita D, Katamine M, Kato A, Katsura A, et al. Impact of triglyceride levels on plaque characteristics in patients with coronary artery disease. International Journal of Cardiology. 2022; 348: 134–139. https://doi.org/10.1016/j.ijcard.2021.12.008

[32] Yang J, Zhou Y, Zhang T, Lin X, Ma X, Wang Z, et al. Fasting Blood Glucose and HbA_{1c} Correlate With Severity of Coronary Artery Disease in Elective PCI Patients With HbA_{1c} 5.7% to 6.4. Angiology. 2020; 71: 167–174. https://doi.org/10.1177/0003319719887655

[33] Liu MM, Peng J, Guo YL, Wu NQ, Zhu CG, Gao Y, et al. Impact of diabetes on coronary severity and cardiovascular outcomes in patients with heterozygous familial hypercholesterolaemia. European Journal of Preventive Cardiology. 2022; 28: 1807–1816. https://doi.org/10.1093/eurjpc/zwab042